引用格式：YANG Xi, YIN Huanhuan, SHAO Zhihua, et al. Ultrasonic Microfiber Sensor Based on Tapered Seven-core Fiber [J]. Acta Photonica Sinica, 2022, 51(3):0306006
杨熙,阴欢欢,邵志华,等.基于锥形七芯光纤的紧凑型超声波传感器[J].光子学报,2022,51(3):0306006

基于锥形七芯光纤的紧凑型超声波传感器

杨熙,阴欢欢,邵志华,乔学光
(西北大学 物理学院, 西安 710069)

摘　要:提出一种基于锥形七芯光纤的紧凑型光纤超声传感器,并进行了实验验证。该传感器由熔接在两根单模光纤之间的锥形七芯光纤制成,形成单模光纤—锥形七芯光纤—单模光纤的级联结构。由于单模光纤和七芯光纤的纤芯不匹配,容易激发高阶模式,被激发的多种模式的光波继续沿着七芯光纤传播,然后到达锥形区域。由于锥度直径的急剧减小,模式间发生干涉,传感器的灵敏度得到提高。制备了不同直径的锥形七芯光纤,并对其模间干涉和超声测量进行了对比分析。超声波在水中传播时,将周期性地改变周围液体的折射率,基于锥形光纤的倏逝场效应,调制锥形光纤中光波的传输。该超声波传感器具有制作简单、信噪比高、频率响应宽等特点。

关键词:光纤传感;光纤超声波传感器;倏逝场;微纳光纤;七芯光纤
中图分类号:TN247　　**文献标识码**:A　　**doi**:10.3788/gzxb20225103.0306006

0 Introduction

Traditional detection approaches usually employ the Piezoelectric Transducers (PZTs) as the signal source and receiver [1]. However, these current-driven transducers have some inherent drawbacks (susceptibility to electromagnetic interference, narrow response frequency band and not resistant to high temperature). Fiber-optic sensors have attracted significant attention in ultrasonic detecting due to their outstanding advantages, such as: anti-electromagnetic interference, small size, easy reuse and bandwidth of response frequency [2].

The majority of fiber-optic ultrasonic sensors are based on Fiber Bragg Gratings (FBGs) [3] and Fabry-Pérot interferometers (FPIs)[4-5]. FBG′s response sensitivity to Ultrasonic Waves (UWs) is determined by reflectivity and spectral bandwidth, when using the spectral filtering technology. LI Yuan et al. proposed an all-fiber multi-channel ultrasonic sensor by using a switchable FBGs filter in an Erbium-Doped Fiber Laser (EDFL). UWs could be detected by monitoring the laser intensity modulation via the ultrasound-induced relative spectral shift of the matched FBGs in the filter[6]. However, the response frequency range of ultrasonic sensors based on FBG is relatively narrow. In addition, FPI sensors are also capable of detecting UWs with high sensitivities. FPI ultrasonic sensors generally consist of a diaphragm and a fiber-optic end-face as two reflectors. The diaphragm materials include polymer, metal films and graphene films, etc. [7-10]. For example, GUO Fanwen et al. proposed a fiber-tip sensor using an ultra-thin silver diaphragm for high-sensitivity and high-frequency ultrasonic detection. The sensor has a 300 nm thick diaphragm on a tube with an inner diameter of 75 μm[11]. The static pressure sensitivity is measured to be 1.6 nm/kPa, and the lowest order resonant

Foundation item: National Natural Science Foundation of China (Nos. 61735014, 61927812, 62005214)
First author: YANG Xi (1996—), female, M.D. degree candidate, mainly focuses on fiber ultrasonic sensing technology. Email: jangyang@stumail.nwu.edu.cn
Contact author: SHAO Zhihua (1987—), male, associate professor, Ph.D. degree, mainly focuses on optical fiber sensing technology. Email: zhshao@nwu.edu.cn
Supervisor (Contact author): QIAO Xueguang (1955—), male, professor, Ph.D. degree, mainly focuses on photonics technology, fiber communication and sensing, fiber sensor system in oil and gas exploration and production, geological exploration, and long-distance oil and gas pipeline leakage detection. Email: xgqiao@nwu.edu.cn
Received: Oct.13, 2021; **Accepted**: Jan.7, 2022

frequency is measured to be 1.44 MHz[11]. However, the complex preparation of diaphragm materials, poor chemical stability and heat resistance limit the sensor's application. In comparison, the inter-mode interference sensors based on Tapered Seven-core Fibers (TSCFs) can be another remarkable candidate for UW detection. The ultrasonic response of the sensor is improved by tapering the sensing fiber.

In this paper, a compact fiber-optic ultrasonic sensor based on TSCFs is proposed and experimentally demonstrated. The tapered region of TSCFs has a strong evanescent field effect, which largely overlaps with the ultrasonic coupling agent (water). The applied ultrasonic field changes the water density and then shifts the interferometric fringe of the transmission spectrum. Herein TSCFs in different diameters are fabricated, and their mode interferences and ultrasonic measurements are comparatively analyzed.

1 Sensor fabrication and principle

The sensor comprises a TSCF sandwiched between two Single-Mode Fibers (SMFs), forming a cascade structure of SMF-TSCF-SMF, as shown in Fig. 1(a). Fig.1(b) shows the waist micrographs of TSCFs with different diameters. In the SMF-TSCF-SMF structure, high order modes are easily excited due to the core mismatch of SMF and Seven-Core Fiber (SCF). Excited multiple modes continue to propagate along the TSCF and then arrive at the tapered region. Due to the sharply reduced taper diameter (as thin as several micrometers), the core distances are largely decreased and the evanescent fields are extended simultaneously[12-13]. Thus, it is sufficient to induce diverse inter-modal coupling at the abrupt taper, including the mode coupling among cores, and coupling and recoupling of the cladding-to-core modes. Finally, most of these fiber modes are coupled back to the SMF, and highly sensitive mode interferences are obtained[14].

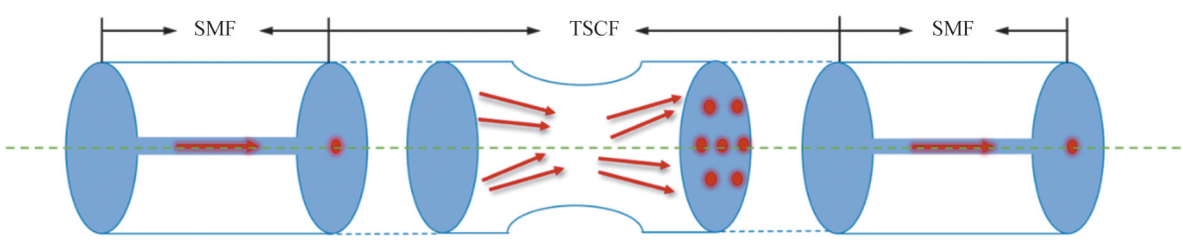

(a) Sensor structure diagram

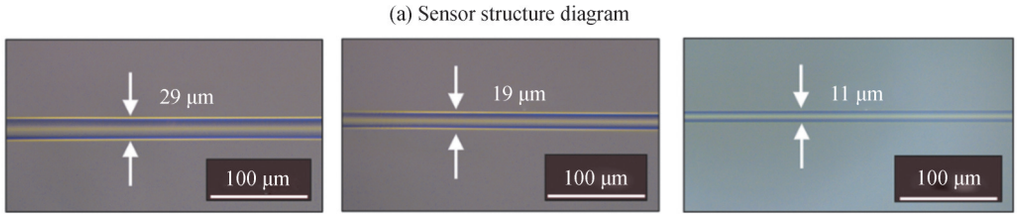

(b) TSCFs micrographs with diameters of 29 μm, 19 μm and 11 μm

Fig. 1 The proposed TSCF sensor

A commercial fiber fusion machine (Fujikura, FSM-80C) is used to fabricate the SMF-TSCF-SMF structure with a 9-mm-long seven-core fiber. Then a fiber flame taper (FBT-Zolix) is used to taper the SCF into TSCF in different diameters. A certain prestress is applied to keep the SCF tight and straight during the fused tapering process. To obtain a uniform and symmetrical TSCF, the tapering step is divided into two steps: setting the velocity and displacement of sliders to 2.6 mm/s and 0.5 mm, respectively, and then increasing the two drawing parameters to 3.6 mm/s and 2.5 mm separately. The tapering parameters can be adjusted as needed to fabricate TSCFs in different diameters. In this paper, SCF (YOFC, MC1010-A, China) is used to make ultrasonic sensors. The six cores of the seven-core fiber are located on the six corners of the regular hexagon, and the center of the hexagon is the middle core of the seven-core fiber. The diameter of the SCF is 150 μm, and the distance between adjacent cores is 42 μm. Taper fibers are fabricated with diameters of 11 μm, 19 μm and 29 μm, and the micrographs of the tapered areas are shown in Fig. 1(b).

Fig.2 shows the transmission spectra of the SMF-TSCF-SMF structure with taper diameters of 29 μm (black curve), 19 μm (red curve) and 11 μm (blue curve). Owing to the core mismatch at the lead-in junction,

the core-guided fundamental mode from the lead-in SMF is coupled into the cladding and core of the TSCF. According to the inter-mode interference mechanism, when the diameter of TSCF fiber is 29 μm, these excited modes propagate in the cladding and core respectively and finally couple back to the lead-out SMF together with weak core modes. No obvious modal interference is observed in the transmission spectrum of the SMF-SCF-SMF structure (black curve). When the SCF is tapered to be below 20 μm, the closer fiber cores and expanded mode fields enhance the mode excitation and coupling in the TSCF, leading to the typical multi-mode interference in Fig. 2 (red and blue curves). Thus, TSCFs with diameters of 11 μm and 19 μm are typically used in subsequent experiments.

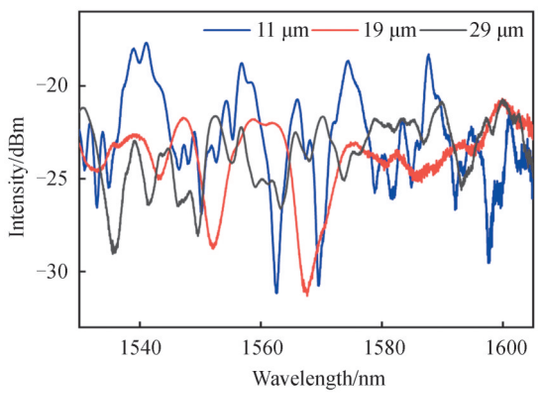

Fig. 2 Transmission spectra of the SMF-TSCF-SMF structure with 29 μm diameter taper, 19 μm diameter taper and 11 μm diameter taper

The transmission spectra of TSCF with diameters of 11 μm and 19 μm in water and air are shown in Fig. 3 As can be seen, the spectra of TSCF before and after water entry change greatly when the diameter of TSCF taper is too small. Therefore, a tapered optical fiber with a diameter of about 19 μm is used as the ultrasonic receiver in this experiment. High order modes are more easily excited because of the taper structure of SCF. As the taper diameter decreases, the transverse modes of the input light expands and couples with the cladding modes. According to the coupled-mode theory[14], the coupling coefficient (K) within the TSCF can be expressed as

$$K=\frac{\lambda^2\left(n_{co}^2-n_{cl}^2\right)^{3/2}\left[\left(\frac{2\pi n_{co}}{\lambda}\right)^2-\beta_p^2\right]k_0}{2\pi n_{co}ak_1^2} \tag{1}$$

where a is one core diameter, λ is the optical wavelength in vacuum, n_{co} and n_{cl} are the effective Refractive Index (RI) of the core and the cladding modes, respectively. k_0 and k_1 represent the modified Bessel functions of the second kind. β_p is the propagation constant. It is clear that the modal excitation and coupling in Figs. 2(a)

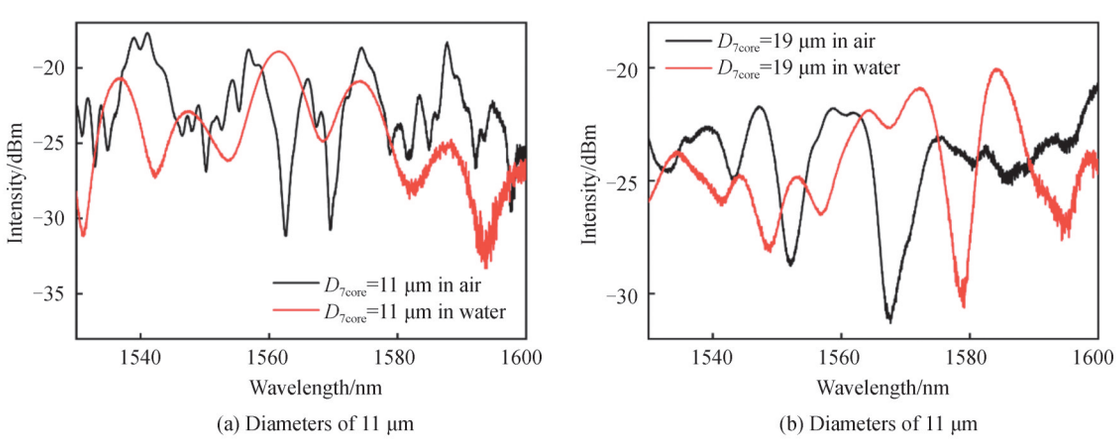

Fig. 3 Transmission spectra of TSCF with different diameters before and after entering water

and (b) largely depend on the taper diameter of the TSCF (proportional to core diameter a). The coupling between TSCF cores increases with the decrease of core distance.

On the other hand, the core and cladding diameters in the tapering region become thinner due to the tapering. The light in core can be transmitted along with the surface of the tapered SCF due to the evanescent wave [15]. When the TSCF is immersed into water, the fundamental guided mode of the microfiber partially spread into the water in the form of evanescent field. The transverse mode field and the corresponding effective index n_{eff} can be changed by varying the RI or density of water, based on the evanescent field interaction. Considering the applied acoustic pressure is weak, the RI of water change can be approximately condemned as linear. Through the first-order Taylor's expansion, the relation between the RI and the acoustic pressure can be given by [16, 17]

$$n_{\mathrm{w}}(p) = n_{\mathrm{w},0} + k(p - p_0) \tag{2}$$

where p is the applied acoustic pressure, $p_0 = 100$ kPa, $k = 1.5 \times 10^{-10}\,\mathrm{Pa}^{-1}$, $n_{\mathrm{w},0} = 1.33$ is the RI of water at static condition. Due to the axial constraints, the axial elongation of the fiber is zero. Therefore, only the index change contributes to the phase change [18]. As the optical signal enters TSCF, multiple modes are excited and coupled. The transmission spectrum of TSCF is the superposition of multiple modes, and the mode field distribution after a propagation length of L in TSCF can be given by [18]

$$E(r, L) = \sum_{m=1}^{M} c_m \psi_m(r) \exp\left(\mathrm{j}\frac{2\pi n_{\mathrm{eff}}}{\lambda} L\right) \tag{3}$$

where $\psi_m(r)$, c_m are the mode field profile, excitation coefficient, and the propagation constant of each mode in TSCF the mode number in TSCF, respectively. M is the mode number in TSCF. Therefore, the change of effective RI of the transmission mode will cause the output intensity of the sensor change. In addition, it has been demonstrated in Refs. [19, 20] that the n_{eff} within the TSCF changes with the external RI. Therefore, the liquid RI ($n_{\mathrm{w}}(p)$) change around the sensor finally results in variation of the output optical intensity.

2 Experimental results and discussions

The fiber-optic ultrasonic detection system is shown in Fig. 4. A tunable laser (Santec, TSL-710) with a 100 kHz linewidth as the light source is launched into the sensor through a fiber. The light power is converted into an electrical signal by a photodetector (PD, New Focus) with a bandwidth of 10 MHz and finally monitored by an oscilloscope (RIGOL, DS2302A). The function generator (OLYMPUS, 5077R) generates a rectangular pulse signal with amplitude of 4 V and repetition frequency of 100Hz to drive the PZT (EasyNDT, 0.5P25SJ, SIUI, 1Z20SJ50DJ, EasyNDT, 5P20SJ). The response characteristics of TSCF to UWs are tested. Experiments are carried out in water for better ultrasonic propagation and coupling. Edge band filtering method is used to demodulate the ultrasonic signal received by TSCF sensor.

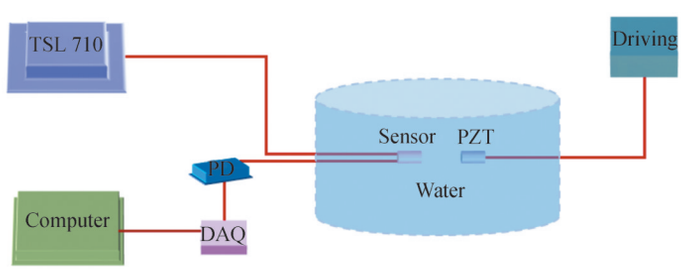

Fig. 4 Schematic diagram of the ultrasonic detection system

As expected, the continuous UW signal presents good uniform and stability in time domain, as shown in Fig. 5(a), where the frequency of PZT is 1 MHz and the amplitude is 4 V, the output power of the tunable laser is 20 mW and the distance between the sensor and PZT is 2.5 cm. Fig. 5(b) shows the time domain response of the TSCF to the UW single. The response amplitude of the TSCF sensor is of about 0.43 V.

To demonstrate the stability of the sensor, the repetition frequency of the signal generator is fixed at 100 Hz and the driving amplitude is 4 V to drive PZT to emit ultrasonic with a frequency of 1MHz. The TSCF sensor response sequence is collected at room temperature, as shown in Fig. 6(a). The corresponding fluctuations of

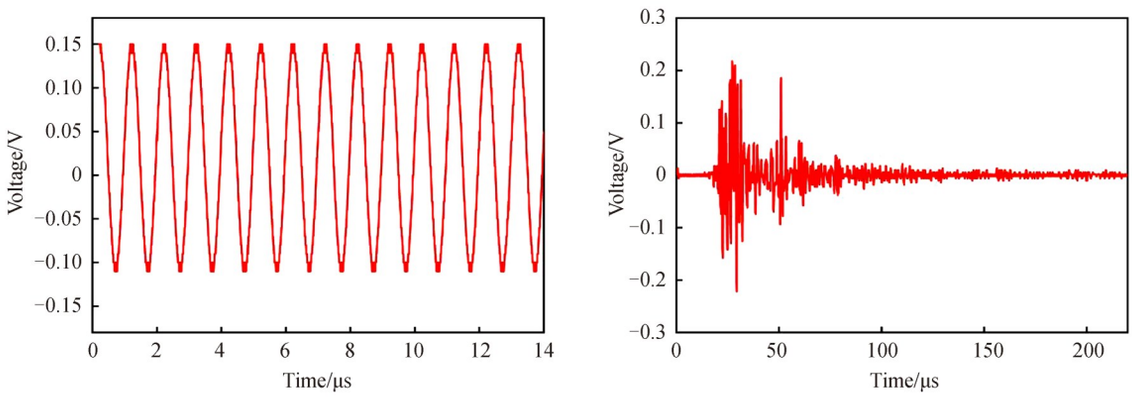

(a) 1 MHz continuous sinusoidal signal sensor ultrasonic response (b) 1 MHz pulse sensor ultrasonic response

Fig. 5 1 MHz sensor ultrasonic response

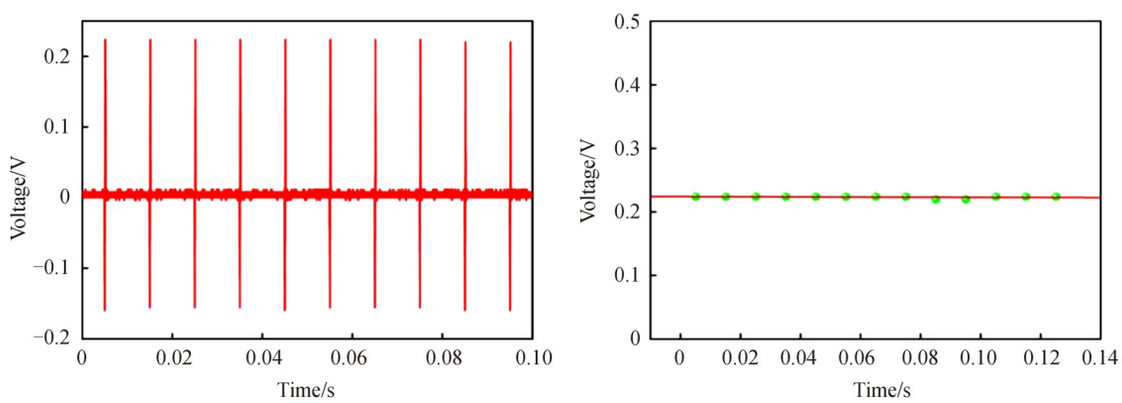

(a) Time domain response sequence to 1 MHz pulsed UW (b) Stability of sensor output signal at room temperature

Fig. 6 Sensor stability test

peak voltages of sensor response signal are shown in Fig. 6(b). The maximum fluctuation of the output voltage is only 0.004 V. Compare with the signal voltage (about 0.224 V), the fluctuation can be neglected. Therefore, the uniform pulse array confirms the sensing stability. The stability and accuracy of wave length and high power of TSL-710 ensure the good stability of the sensing system and the high sensitivity detection of UWs.

The response to UW of sensor is performed at the different distances between PZT and sensor. In the experiment, two devices are hold in the same axis, and the sensor is moved along the axis by moving stage. UWs are recorded in the range of 1 cm to 5 cm with a separation of 0.5 cm. As shown in Fig.7(a), the voltage is 0.43 V when distance between the sensor and the PZT is 3 cm. The voltage signal changes with the distance

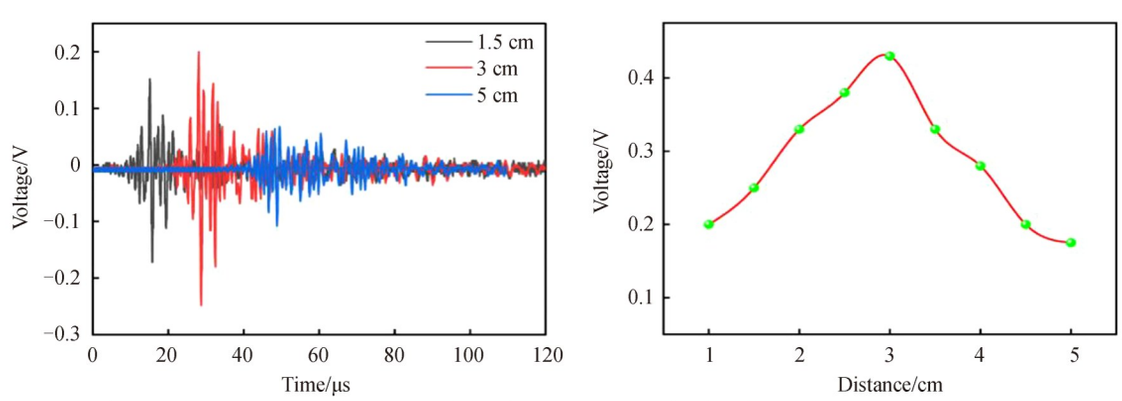

(a) Sensor′s response to a pulse ultrasound signal (b) The relationship between the distance between the PZT and the sensor and the signal peak value

Fig. 7 Experimental measurement

change between PZT and the sensor as shown in Fig. 7(b), which increases at first and then decreases. The main reason is that the PZT used in the experiment is a focused emission source with a focal length of 3 cm. The UW focuses on the sensor when the distance between PZT and sensor is the PZT focal length, and the sensor receives the maximum ultrasonic energy. When the distance between sensor and PZT is not equal to the focal length of PZT, the UW energy received by the sensor is greatly reduced.

The sensor also measures UWs at several frequencies of 250 kHz and 5 MHz, and the results are shown in Fig. 8. These experimental results show that the sensor has good ability to measure broadband UWs. Fourier transform is used to convert the time domain signal of the sensor into spectrum information. As shown in Fig. 9, the main frequencies of 500 kHz and 5 MHz are consistent with the actual PZT transmission frequency.

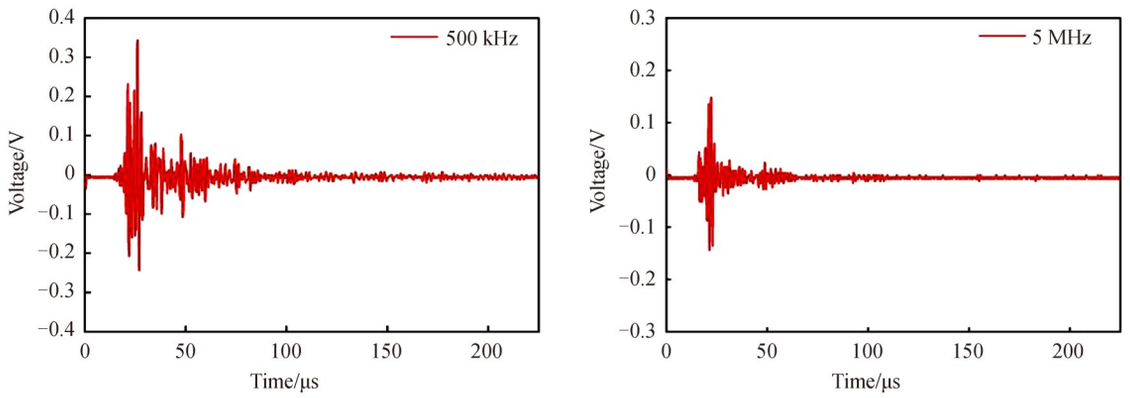

(a) Sensor response to UWs with frequency of 500 kHz (b) Sensor response to UWs with frequency of 5 MHz

Fig. 8 Ultrasonic response of sensor

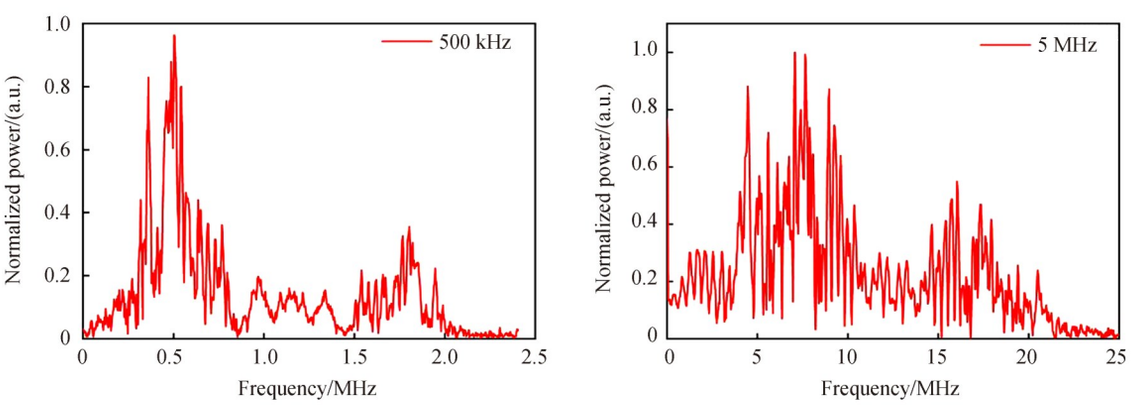

(a) 500 kHz (b) 5 MHz

Fig. 9 Spectrum response characteristics of sensor to pulsed UWs with frequency of 500 kHz and 5 MHz

The change of sensor time domain signal with PZT driving voltage is shown in the Figs. 10. PZT voltage

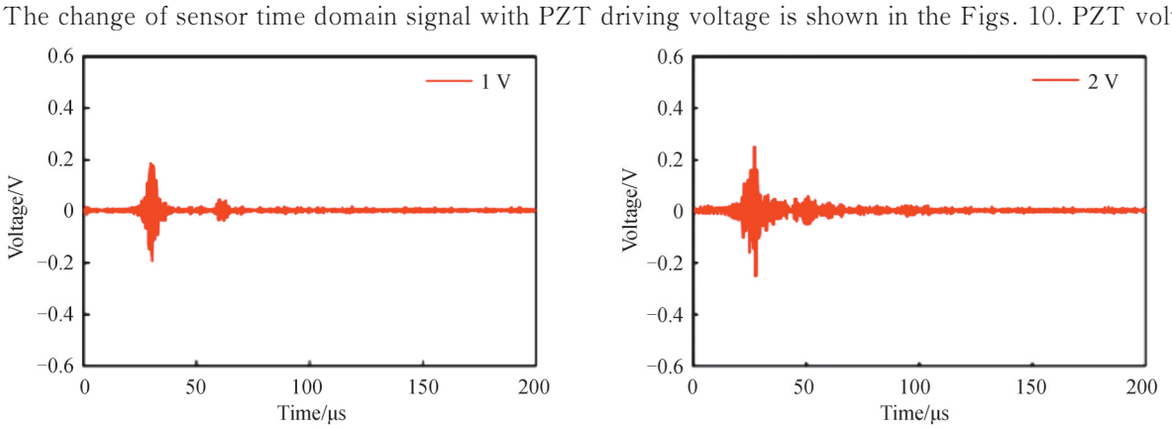

(a) PZT driving voltage is 1 V (b) PZT driving voltage is 2 V

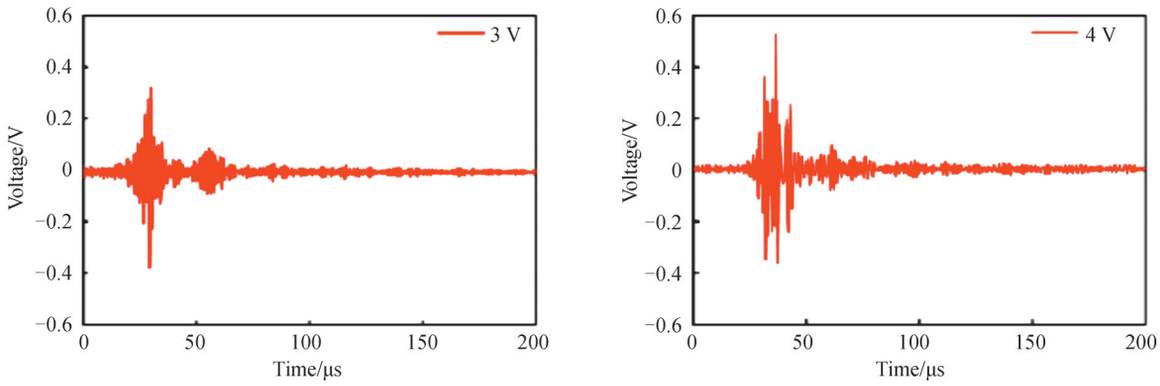

(c) PZT driving voltage is 3 V (d) PZT driving voltage is 4 V

Fig. 10 Variation of sensor response amplitude with ultrasonic intensity

gradually increases from 1 V to 4 V, and the amplitude of ultrasonic signal received by the sensor is also gradually increasing.

3 Conclusion

In conclusion, a compact fiber-optic taper sensor based on Tapered Seven-Core Fiber (TSCF) is designed for high frequency Ultrasonic Wave (UW) detection. Due to the tapered region of TSCFs has a strong evanescent field effect, when placing the sensor in water, the UW signal periodically changes the refractive index of the surrounding liquid and modulates the transmission spectrum according to the evanescent-field interaction between the liquid and the transmitting light. The TSCF with different diameter is analyzed theoretically, and the TSCF with region diameter of 19 μm is selected for experimental test. By testing the response of the TSCF to ultrasonic signals with different frequencies and intensities, it is proved that the sensor has good ultrasonic response characteristics.

References

[1] BUDDENSIEK M L, KRAWCZYK C M, KUKOWSKI N, et al. Performance of piezoelectric transducers in terms of amplitude and waveform[J]. Geophysics, 2009, 74(2): 33-45.

[2] LIN Shuyu, WANG Shuaijun. Radially composite piezoelectric ceramic tubular transducer in radial vibration[J]. IEEE transactions on ultrasonics, ferroelectrics, and frequency control, 2011,58(11): 2492-2498.

[3] WU Qi, OKABE Y. Waveform reconstruction for an ultrasonic fiber Bragg grating sensor demodulated by an erbium fiber laser[J]. Applied Optics, 2015, 54(4):694-698.

[4] QIAO Xueguang, SHAO Zhihua, BAO Weijia, et al. Fiber-optic ultrasonic sensors and applications[J]. Acta Physica Sinica, 2017, 66(7): 128-147.

[5] RONG Qiangzhou SHAO Zhihua, YIN Lixun, et al. Ultrasonic imaging of seismic physical models using fiber bragg grating Fabry - Perot probe[J]. IEEE Journal of Selected Topics in Quantum Electronics, 2017, 23(2): 223-228.

[6] LI Yuan, TIAN Jiajun, QI Fu, et al. A multi-point switchable and self-adaptive ultrasonic sensor using fiber Bragg gratings in a fiber ring laser[J]. Journal of Lightwave Technology, 2018, 37(4): 1160-1167.

[7] GONG Zhenfeng, CHEN Ke, ZHOU Xinlei, et al. High-sensitivity Fabry-Perot interferometric acoustic sensor for low-frequency acoustic pressure detections[J]. Journal of Lightwave Technology, 2017, 35(24): 5276-5279.

[8] CHEN Jinhui, LI Danran, XU Fei. Optical microfiber sensors: sensing mechanisms, and recent advances[J]. Journal of Lightwave Technology, 2018, 37(11): 2577-2589.

[9] WANG Qiaoyun, YU Qingxu. Polymer diaphragm based sensitive fiber optic Fabry-Perot acoustic sensor[J]. Chinese Optics Letters, 2010, 8(3):266-269.

[10] JIANG Junfeng, ZHANG Tianhao, WANG Shuang, et al. Noncontact ultrasonic detection in low-pressure carbon dioxide medium using high sensitivity fiber-optic Fabry - Perot sensor system[J]. Journal of Lightwave Technology, 2017, 35(23): 5079-5085.

[11] GUO Fawen, FINK T, HAN Ming, et al. High-sensitivity, high-frequency extrinsic Fabry-Perot interferometric fiber-tip sensor based on a thin silver diaphragm[J]. Optics Letters, 2012, 37(9): 1505-1507.

[12] WANG Xiaoliang, CHEN Daru, LI Haitao, et al. In-line Mach-Zehnder interferometric sensor based on a seven-core optical fiber[J]. IEEE Sensors Journal, 2016, 17(1): 100-104.

[13] XU Ben, LI Yi, SUN Miao, et al. Acoustic vibration sensor based on nonadiabatic tapered fibers[J]. Optics Letters, 2012, 37(22): 4768-4770.
[14] YOON M S, LEE S B, HAN Y G. In-line interferometer based on intermodal coupling of a multicore fiber[J]. Optics Express, 2015, 23(14): 18316-18322.
[15] FU Xinghu, XIU Yanli, LIU Qin, et al. Refractive index sensors based on the fused taper special multi-mode fiber[J]. Optoelectronics Letters, 2016, 12(1): 12-15.
[16] WANG Xiuxin, JIN Long, LI Jie, et al. Microfiber interferometric acoustic transducers[J]. Optics Express, 2014, 22(7):8126-8135.
[17] WURSTER C, STAUDENRAUS J, EISENMENGER W. The fiber optic probe hydrophone [C]. Ultrasonics Symposium IEEE, 1994, 2: 941-944.
[18] SNYDER A W. Coupled-mode theory for optical fibers[J]. Journal of the Optical Society of America, 1972, 62(11): 1267-1277.
[19] ZHANG Chuanbiao, NING Tigang, LI Jing, et al. Refractive index sensor based on tapered multicore fiber[J]. Optical Fiber Technology, 2017, 33: 71-76.
[20] SHAO Zhihua, QIAO Xueguang, RONG Qiangzhou. Highly sensitive gas refractometer based on inverse mode-coupling of cladding-to-core modes in a tapered four-core fiber[C]. Optical Fiber Sensors Conference IEEE, 2017: 1-4.

Ultrasonic Microfiber Sensor Based on Tapered Seven-core Fiber

YANG Xi, YIN Huanhuan, SHAO Zhihua, QIAO Xueguang
(*School of Physics, Northwest University, Xi'an* 710069, *China*)

Abstract: Traditional detection approaches usually employ Piezoelectric Transducers (PZTs) as the ultrasonic source and receiver. However, these current-driven transducers have some inherent drawbacks (susceptibility to electromagnetic interference, narrowband frequency response, and not resistant to high temperature and corrosion). Fiber-optic sensors have attracted significant attention in ultrasonic detecting owing to their outstanding advantages, such as: small size, easy reuse, wideband frequency response, and immunity to electromagnetic interference. The majority of fiber-optic ultrasonic sensors has based on fiber Bragg gratings and Fabry-perot interferometers. However, frequency response range of ultrasonic sensors based on FBGs is relatively narrow. The Fabry-perot interferometers ultrasonic sensors generally consist of a diaphragm and a fiber-optic end-face as two reflectors. Nevertheless, the complex preparation of diaphragm materials, poor chemical stability, and heat resistance, limit the application of sensor. In this study, a compact fiber-optic ultrasonic sensor based on a Tapered Seven-core Fiber (TSCF) is proposed and experimentally demonstrated. This proposed sensor has the advantages of easy fabrication, compact structure, and high sensitivity. The sensor comprises a TSCF sandwiched between two Single-mode Fibers (SMFs), forming a cascade structure of SMF-TSCF-SMF. The SCF (YOFC, MC1010-A, China) is used to make ultrasonic sensors. A commercial fiber fusion splicer (Fujikura, FSM-80C) is used to fabricate the SMF-TSCF-SMF structure. Thereafter, the optical fiber fused biconical taper system (FBTZolix) is used to taper the SCF into the TSCF with diameters of 11 μm, 19 μm and 29 μm. A certain prestress is applied to keep the SCF tight and straight during the fused tapering process. High order modes are easily excited owing to the core mismatch of SMF and Seven-core Fiber (SCF). The excited multiple modes continue to propagate along the SCF and then arrive at the tapered region. These transmission spectra exhibited multiple interference peaks. This is because complex optical modes are excited and are involved in mode interference. Therefore, these transmission spectra are not in a standard sinusoidal pattern, but become more irregular. Due to the sharply reduced taper diameter (as thin as several micrometers), the core distances are largely decreased and the evanescent fields are extended simultaneously. Thus, it is sufficient to induce diverse inter-modal coupling at the abrupt taper, including the mode coupling among cores, and coupling and recoupling of the cladding-to-core modes. Highly sensitive mode interferences are obtained. For the TSCF, the ultrasonic wavelength is much longer than the taper diameter and shorter than the fiber length. The fiber taper is axially constrained, that is, the axial elongation of the fiber taper can be neglected. The core and cladding diameters in the tapered region become

thinner, and the TSCF has an obvious effect on evanescent waves. When the sensor is immersed in water, the Ultrasonic Wave (UW) signal periodically changes the refractive index of the surrounding liquid and modulates the transmission spectrum according to the evanescent-field interaction between the liquid and the transmitting light. Meanwhile, due to the effect of evanescent field, the light energy transmitted in the fiber can penetrate into the surrounding medium, resulting in energy reduction. Thus, the TSCF sensor with a diameter taper of 19 μm is used as the receiving source of ultrasonic signals. Driven by a function generator, the PZT (SIUI, 1Z20SJ50DJ) separately emits a 1 MHz continuous wave with a voltage amplitude of 10 V as the ultrasonic source. The edge filtering method is used to demodulate the ultrasonic signal received by the TSCF sensor. A tunable laser (Santec-710) with a 100 kHz linewidth and 0.1 pm tunable resolution was used as the light source. The output power of the tunable laser was 20 mW. The photodetector (New Focus, Model 2117) with a bandwidth of 10 MHz converts the optical signal into a voltage signal, which is finally monitored by an oscilloscope (RIGOL, DS2302A). The bandpass filter built into the photodetector has a frequency range of 500 kHz to 3 MHz, which is used to shield the surrounding noise. UW detection is processed in water at room temperature, which provides an almost constant temperature environment around the sensor. The sensor directly faces the emitting end of PZT with a separation of 2.5 cm. The continuous signals exhibit good uniformity and stability in the time domain. The peak-to-peak voltage of TSCF is about 0.4 V.

Key words: Fiber sensor; Ultrasonic fiber sensor; Microfiber; Seven-core fiber; Evanescent field

OCIS Codes: 060.2370; 280.4788; 170.7170